HOKKAIDO UNIVERSITY

Title	Behavior of intermolecular interactions in alpha-glycine under high pressure
Author(s)	Shinozaki, Ayako; Komatsu, Kazuki; Kagi, Hiroyuki et al.
Citation	Journal of chemical physics, 148(4), 044507 https://doi.org/10.1063/1.5009980
Issue Date	2018-01-28
Doc URL	https://hdl.handle.net/2115/72388
Rights	The following article appeared in The Journal of Chemical Physics 148, 044507 2018 and may be found at doi:10.1063/1.5009980
Type	journal article
File Information	JCP148 044507.pdf

Hokkaido University Collection of Scholarly and Academic Papers : HUSCAP

Behavior of intermolecular interactions in α-glycine under high pressure

Ayako Shinozaki, Kazuki Komatsu, Hiroyuki Kagi, Chikako Fujimoto, Shinichi Machida, Asami Sano-Furukawa, and Takanori Hattori

Citation: The Journal of Chemical Physics **148**, 044507 (2018); doi: 10.1063/1.5009980
View online: https://doi.org/10.1063/1.5009980
View Table of Contents: http://aip.scitation.org/toc/jcp/148/4
Published by the American Institute of Physics

Articles you may be interested in

An atomistic fingerprint algorithm for learning ab initio molecular force fields
The Journal of Chemical Physics **148**, 034101 (2018); 10.1063/1.5008630

Kinetic boundaries and phase transformations of ice i at high pressure
The Journal of Chemical Physics **148**, 044508 (2018); 10.1063/1.5017507

Perspective: Quantum Hamiltonians for optical interactions
The Journal of Chemical Physics **148**, 040901 (2018); 10.1063/1.5018399

B97-3c: A revised low-cost variant of the B97-D density functional method
The Journal of Chemical Physics **148**, 064104 (2018); 10.1063/1.5012601

Benchmarking several van der Waals dispersion approaches for the description of intermolecular interactions
The Journal of Chemical Physics **148**, 064112 (2018); 10.1063/1.5018818

Classical molecular dynamics simulation of microwave heating of liquids: The case of water
The Journal of Chemical Physics **148**, 024508 (2018); 10.1063/1.5001928

AIP | The Journal of Chemical Physics
PERSPECTIVES

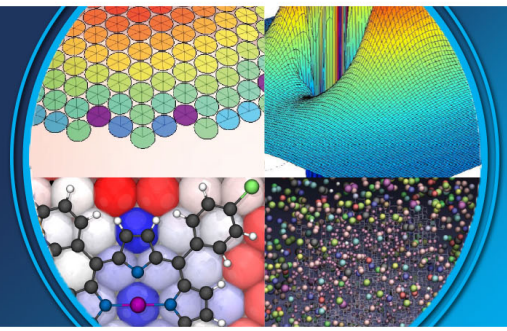

Behavior of intermolecular interactions in α-glycine under high pressure

Ayako Shinozaki,[1,a)] Kazuki Komatsu,[2] Hiroyuki Kagi,[2] Chikako Fujimoto,[2] Shinichi Machida,[3] Asami Sano-Furukawa,[4] and Takanori Hattori[4]
[1]*Faculty of Science, Hokkaido University, Kita 10 Nishi 8, Kita-ku, Sapporo, Hokkaido 060-0810, Japan*
[2]*Geochemical Research Center, Graduate School of Science, The University of Tokyo, Hongo, Tokyo 113-0033, Japan*
[3]*CROSS, Neutron Science and Technology Center, IQBRC Building, 162-1 Shirakata, Tokai, Ibaraki 319-1106, Japan*
[4]*J-PARC Center, Japan Atomic Energy Agency, 2-4 Shirakata, Tokai, Ibaraki 319-1195, Japan*

(Received 21 October 2017; accepted 5 January 2018; published online 26 January 2018)

Pressure-response on the crystal structure of deuterated α-glycine was investigated at room temperature, using powder and single-crystal X-ray diffraction, and powder neutron diffraction measurements under high pressure. No phase change was observed up to 8.7 GPa, although anisotropy of the lattice compressibility was found. No significant changes in the compressibility and the intramolecular distance between non-deuterated α-glycine and deuterated α-glycine were observed. Neutron diffraction measurements indicated the distance of the intermolecular D···O bond along with the *c*-axis increased with compression up to 6.4 GPa. The distance of another D···O bond along with the *a*-axis decreased with increasing pressure and became the shortest intermolecular hydrogen bond above 3 GPa. In contrast, the lengths of the bifurcated N–D···O and C–D···O hydrogen bonds, which are formed between the layers of the α-glycine molecules along the *b*-axis, decreased significantly with increasing pressure. The decrease of the intermolecular distances resulted in the largest compressibility of the *b*-axis, compared to the other two axes. The Hirshfeld analysis suggested that the reduction of the void region size, rather than shrinkage of the strong N–D···O hydrogen bonds, occurred with compression. *Published by AIP Publishing.* https://doi.org/10.1063/1.5009980

I. INTRODUCTION

The intermolecular interactions of organic molecules change drastically with compression, leading to pressure-induced structural changes and chemical reactions (e.g., Refs. 1–9). Amino aids, also known as the building blocks of proteins, contain both the amino and carboxyl groups. Amino acids crystallize as zwitterions (e.g., Refs. 4, 10, and 11), forming robust head-to-tail chains of intermolecular hydrogen bonds, namely, N–H···O bonds between the amino group and carboxyl group. In addition, other types of intermolecular hydrogen bonds are formed with the side chains, such as C–H···O bonds. The effect of pressure on the crystal structure and intermolecular interactions has been investigated for several amino acids, such as L-, DL-alanine,[12–15] L-serine,[16–20] and L-, DL-cysteine.[21–24] Recently, the pressure-induced oligomerization of L-alanine at room temperature was reported.[25,26] The oligomerization might occur partially when distances between the neighboring L-alanine molecules decrease with increasing pressure and finally approaches the reaction threshold.[25] However, the detailed mechanism of the oligomerization has not been revealed. Investigation of the effects of pressure on the intermolecular interactions in amino acid crystals may provide essential information regarding the mechanism of the pressure-induced oligomerization of amino acids.

Glycine (H_2NCH_2COOH), the simplest amino acid, has three polymorphs of solid phase at ambient pressure, derived from the geometry of molecular association. The crystal structure of α-glycine obtained by the evaporation of aqueous solution is monoclinic ($P2_1/n$).[27–30] The molecules are linked by the intermolecular hydrogen bonds in antiparallel double-layers.[29–31] β-glycine, crystallized from a water/ethanol solution, has a different monoclinic structure, $P2_1$,[32,33] with a layered structure of the molecules. The most stable form at ambient pressure is γ-glycine,[34–36] crystallized from an acidified solution, and has a trigonal structure, $P3_1$ or $P3_2$. In γ-glycine, the molecules are arranged in helixes linked to each other in a three-dimensional network.[4,31,37] The structural changes of each phase under high pressure have been investigated. X-ray diffraction (XRD) measurements indicated that α-glycine is stable up to at least 6 GPa with no structural changes.[31,38] Raman spectroscopy suggested that the crystal structure of α-glycine persists up to ~23 GPa, although a subtle structural rearrangement was observed at ~3 GPa.[39,40] A high pressure heavier of α-glycine was also investigated using incoherent inelastic neutron scattering up to 1 GPa.[41] In contrast, β-glycine reversibly transforms into a structurally related high-pressure phase at 0.76 GPa without any damage to the single crystal,[38,42] and γ-glycine transforms into another high-pressure phase with a single crystal completely ruined into powder.[38,43–45] On partial decompression, this second

a)Author to whom correspondence should be addressed: shinozaki.aya@sci.hokudai.ac.jp. Tel.: +81-(0)11-706-2727. Fax: +81-(0)11-746-0394.

high-pressure phase gives another, the third one, high-pressure polymorph before having transformed to α-glycine at ambient pressure.[46,47]

In this study, both powder and single-crystal XRD measurements were performed to investigate the high-pressure behavior of deuterated α-glycine. Furthermore, powder neutron diffraction measurements were carried out at high pressure to obtain more accurate positions of hydrogen atoms in the structure, in order to investigate the behavior of the intermolecular hydrogen bonds with compression.

II. EXPERIMENTS

The entire series of experiments were performed using fully deuterated α-glycine (D_2NCD_2COOD, 98.4 at. % D, CDN isotopes, Inc.). The molecular structure and the numbering scheme are shown in Fig. 1. A 4:1 mixture of deuterated methanol:ethanol was used as the pressure medium. The fully deuterated sample and the pressure medium were used to avoid high background caused by incoherent scattering of hydrogen atoms in hydrogenated α-glycine in the neutron diffraction measurements.

Powder XRD patterns were collected with increasing the pressure at room temperature in two runs, up to 8.7 GPa (run 1-1) and 5.5 GPa (run 1-2). A diamond anvil cell (DAC) with a pair of diamond anvils of 450-μm culets was used as a high-pressure device. Stainless steel or Re gaskets were used after pre-compression to ~100 μm in thicknesses. A sample hole with ~200 μm diameter was drilled in the gasket. The pressure was measured using the ruby fluorescence method.[48] XRD patterns were measured at BL-18C of the Photon Factory of the High Energy Accelerator Research Organization (KEK), Ibaraki, Japan. A typical X-ray wavelength was 0.6106 Å, calibrated by the lattice parameter of the CeO_2 standard. The X-ray beam was collimated to 60 μm or 100 μm in diameter. Angle-dispersive XRD patterns were collected with an imaging plate, and the typical exposure time was 10 min. Each XRD image was integrated into a 1D pattern as a function of 2θ using an IP analyzer[49] and then evaluated by the Le Bail fitting method using the GSAS-EXPGUI package.[50]

A single-crystal XRD pattern was collected at 4.1 GPa and room temperature, using the DAC (run 2). The X-ray beam was generated by a microfocused X-ray generator (MicroMax-007; Rigaku) with a Mo rotating target ($\lambda = 0.7107$ Å, 50 kV, 24 mA). The incident X-ray beam was collimated by a single pinhole collimator with a diameter of 300 μm. The diffraction pattern was collected on an imaging plate (R-AXISIV^{++}; Rigaku). We used atomic positions reported

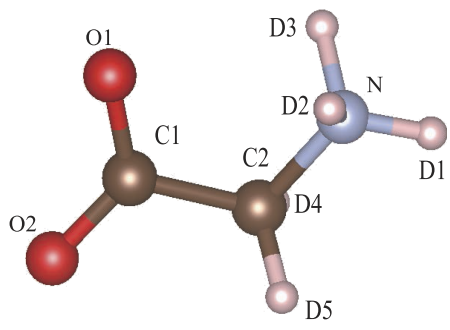

FIG. 1. Molecular structure of α-glycine and the numbering scheme used in this study.

TABLE I. Experimental detail of the single-crystal X-ray diffraction measurement (run 2).

	α-glycine ($C_2D_5NO_2$)
Pressure (GPa)	4.1
Cell setting	Monoclinic
Space group	$P2_1/n$
a (Å)	4.923 (3)
b (Å)	11.266 (2)
c (Å)	5.409 (2)
β (deg)	116.108 (19)
V (Å^3)	269.6 (2)
Z	4
μ (mm^{-1})	0.160
Reflections collected	420
Reflections unique	255
No. of parameters	37
R_{int}	0.0218
R_1 ($I > 2\sigma(I)$)	0.0921
wR_2	0.3165
S	1.644

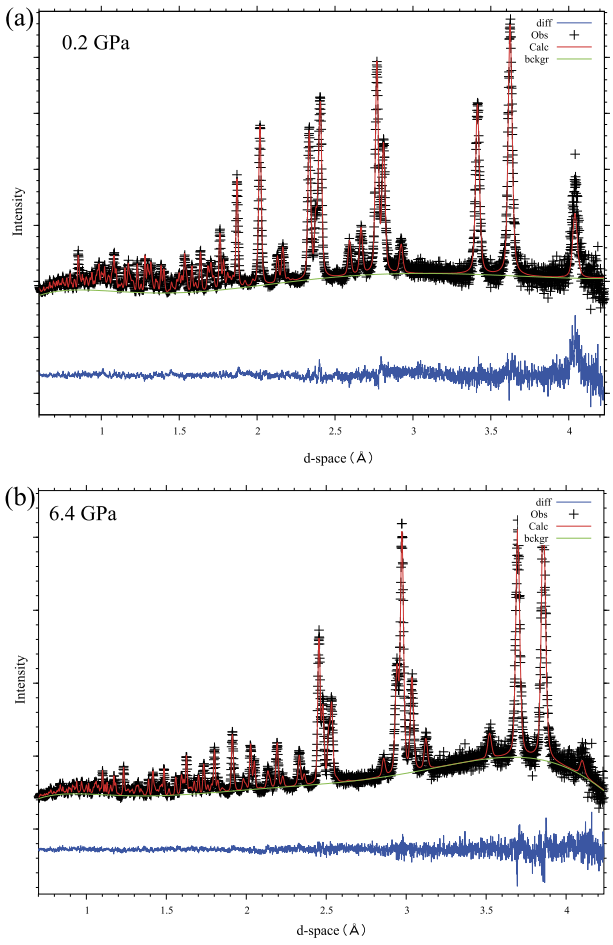

FIG. 2. Rietveld fitting result of the neutron powder diffraction patterns at (a) 0.2 GPa and (b) 6.4 GPa. Black points: observed data, red line: calculated profile, green line: baseline, blue line: the difference.

TABLE II. Representative Rietveld fitting results and experimental details of neutron diffraction measurements.

Pressure (GPa)	0.2	1.3	2.2	3.9	4.4	5.7	6.4
Run no.	Run 3-3	Run 3-3	Run 3-1	Run 3-3	Run 3-2	Run 3-3	Run 3-2
a (Å)	5.087 63 (17)	5.026 65 (17)	4.986 59 (17)	4.924 77 (14)	4.908 43 (15)	4.874 30 (12)	4.860 76 (17)
b (Å)	11.879 4 (3)	11.650 9 (3)	11.516 5 (3)	11.304 2 (3)	11.244 0 (2)	11.116 6 (2)	11.061 5 (3)
c (Å)	5.463 19 (16)	5.447 87 (15)	5.435 04 (17)	5.411 19 (14)	5.402 43 (13)	5.383 30 (14)	5.374 20 (19)
β (deg)	112.086 (3)	113.525 (3)	114.467 (3)	115.819 (2)	116.144 (2)	116.785 (3)	117.051 (3)
V (Å^3)	305.957 (11)	292.540 (10)	284.098 (9)	271.172 (9)	267.660 (8)	260.401 (6)	257.346 (6)
R_{wp}	0.039 8	0.037 1	0.030 1	0.034 4	0.029 6	0.034 3	0.039
R_p	0.045 5	0.044 8	0.037 6	0.041 5	0.034 3	0.041 8	0.048 5
$R(F^2)$	0.096 4	0.072 6	0.029 1	0.065 5	0.069 7	0.058 4	0.078 9
χ^2	0.995 8	0.948 7	1.209	1.312	1.944	1.533	2.349

in Jönsson and Kvick[29] as the initial structure model for the refinement, and all atoms excluding the D atoms were refined using SHEXL-97. The experimental details are listed in Table I.

Three runs of the neutron diffraction measurements (runs 3-1, 3-2, and 3-3) were performed using the time-of-flight technique at the BL11 beamline PLANET,[51] in the Material and Life Science Experimental Facility (MLF) of J-PARC, Ibaraki, Japan. A VX4-type Paris-Edinburgh press,[52] combined with tungsten carbide φ9-6 non-toroidal anvils[53] and single-toroidal anvils, was used to compress the sample. The powdered sample was loaded in a pair of TiZr-encapsulating gaskets, together with the pressure medium (a 4:1 mixture of deuterated methanol:ethanol). The applied pressure was determined from the lattice parameters of α-glycine, using the equation of state (EOS) determined by the powder XRD measurements in the present study. The typical exposure time was 6 h.

The crystal structure was refined using neutron diffraction patterns obtained from 0.2 to 6.4 GPa by the Rietveld method with the GSAS-EXPGUI package.[50] The initial structure model for the refinement was taken from Jönsson and Kvick.[29] Lattice parameters, N, O, C, and D atom positions, and their atomic displacement factors were refined, whereas the U_{iso} values were constrained to be identical for the five D atoms and for the other atoms (C, O, N). Absorption parameters were refined using the data at the lowest pressure in each run, and the determined values were fixed for the data refinement at higher pressures in the same run. The C1–O1, C1–O2, C1–C2, and N1–C2 bond lengths were restrained to those determined by the single-crystal XRD analysis in the present study. The representative results of the Rietveld refinements are shown in Fig. 2 and Table II. The crystal structure was visualized using the VESTA program.[54]

III. RESULTS

Figure 3 shows representative powder XRD patterns for deuterated α-glycine with compression up to 8.7 GPa (run 1-1). All the patterns were indexed as a monoclinic structure ($P2_1/n$). Figure 4 shows the pressure dependence of the lattice parameters, and unit cell volumes, which were comparable with the respective values of undeuterated α-glycine.[31,38] No obvious discontinuity was observed in each parameter with the increase of pressure, suggesting that there is no phase transition in this pressure range. The unit cell volume at ambient pressure (V_0), bulk modulus (K_0), and its pressure derivative (K') were determined to be 309.0(6) Å^3, 19.5(7) GPa, and 6.5(4), respectively, by fitting with the Vinet EOS.[55] Fitting to the Birch-Murnaghan equation[56] was also tested for the obtained data, but no convergence was achieved. The determined bulk modulus of α-glycine was slightly larger than that of L-alanine.[12,14] The *a*, *b*, and *c*-axes were compressed by 5.6%, 8.5%, and 2.2%, respectively, up to 8.7 GPa, indicating anisotropic compressibility. In addition, c'/c'_0 is plotted in Fig. 4(a). c' is defined as a vertical axis to the *ab*-plane and which could indicate the objective changes of the *c*-axis, excluding the influence of the β angle that increases with the compression [Fig. 4(b)]. The c'-axis was compressed by 6.6% up to 8.7 GPa.

Table III lists intramolecular bond lengths and angles obtained from the single-crystal XRD measurement at 4.1 GPa (run 2). The parameters are comparable with previous results obtained by the neutron diffraction measurement at ambient pressure[29] and single-crystal XRD measurements up to 6.2 GPa.[38] The results show that the intramolecular bond lengths and the angles do not change significantly with increasing pressure, at least up to 6 GPa. The N1–C2–C1–O2 torsion

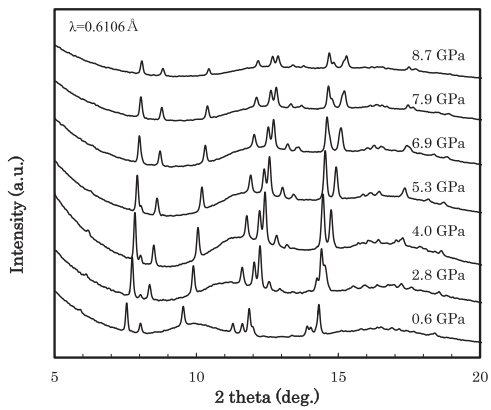

FIG. 3. Representative XRD patterns of α-glycine at high pressure and room temperature.

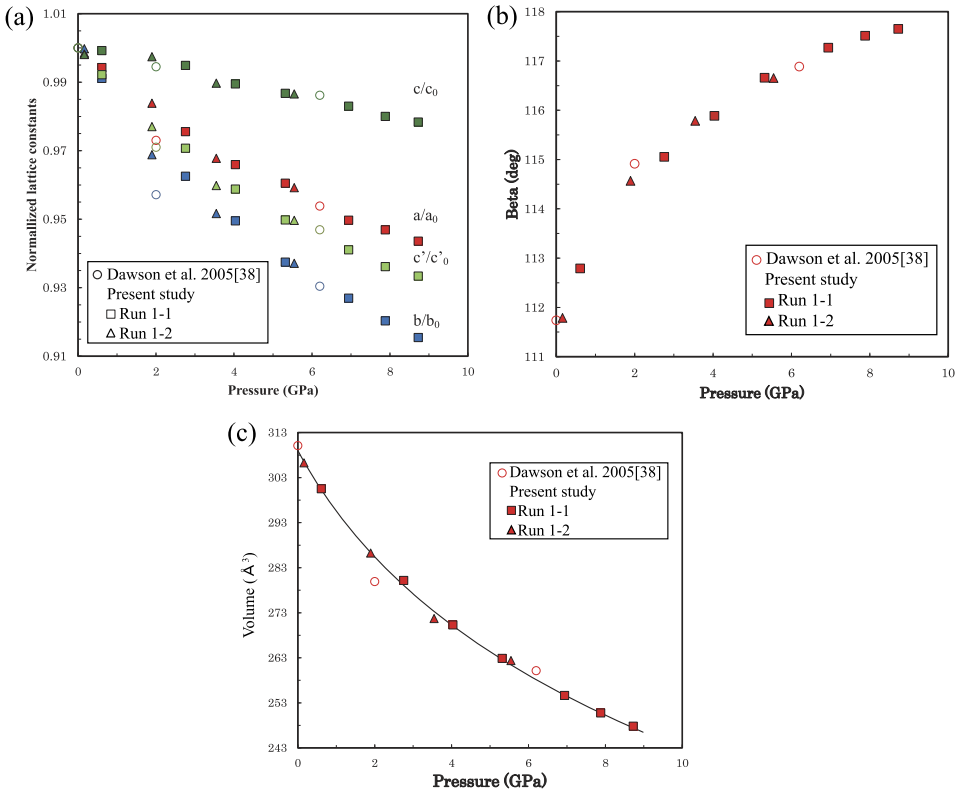

FIG. 4. Pressure dependence of the lattice parameters of α-glycine determined by powder XRD measurements. (a) Length of each axis normalized by the value at ambient pressure, (b) β angle, and (c) unit cell volume and the results of fitting with Vinet EOS. The c'/c'_0 is defined as the normalized length of an axis which is vertical to the *ab*-plane. Solid square, run1-1; solid triangle, run1-2; and open circle, the values from Dawson *et al.*[19]

angle is −13.7° at 4.1 GPa, which is keeping with the trend of that reported by Dawson *et al.*[38] No significant changes in the intramolecular distances, angles, and torsion angles were reported upon compression for L-alanine and L-α-glutamine as well.[12,57]

The intermolecular distances were determined by neutron diffraction measurements. The D1···O1 and D2···O2 intermolecular hydrogen bonds, which are almost along the *c*-axis and the *a*-axis, respectively (Fig. 5), consist of two head-to-tail chains of the C(5) motif[58] in the *ac*-plane. Pressure dependences of the intermolecular D···O distances, consisting of the C(5) chains, are shown in Fig. 6(a), and the representative parameters of the intermolecular hydrogen bonds are listed in Table IV. The D1···O1 distances are almost constant at pressures below 2 GPa, and increased in the pressure range 2–6 GPa, though the D1···O1 distances are scattered depending on the experimental runs. The N···O1 distance is almost constant up to 5.7 GPa, and the N–D1 distance decreases from 1.044(6) Å at 2.2 GPa to 1.000(7) Å at 4.4 GPa. The N–D1···O1 bond angle decreases from 168.8°

TABLE III. Intramolecular distances, bond angles, and torsion angles of deuterated α-glycine determined by the single crystal X-ray diffraction measurement (run 2).

	1 atm[29]	4.1 GPa
C1–O1 (Å)	1.250 (1)	1.254 (5)
C1–O2 (Å)	1.251 (1)	1.245 (9)
C1–C2 (Å)	1.526 (1)	1.516 (7)
C2–N1 (Å)	1.476 (1)	1.476 (10)
C2–C1–O2 (deg)	117.46 (6)	118.0 (4)
C2–C1–O1 (deg)	117.09 (7)	116.9 (4)
N–C2–C1 (deg)	111.85 (5)	111.5 (4)
τN1–C2–C1–O1 (deg)	−19.63 (11)	−13.7 (7)

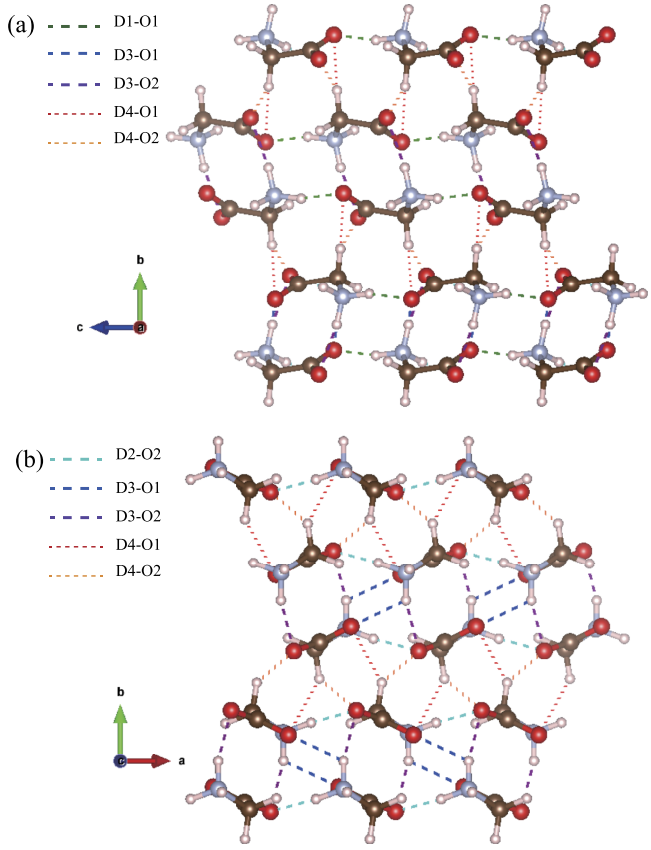

FIG. 5. The crystal structure of α-glycine at 6.4 GPa determined by Rietveld refinement of the neutron diffraction pattern. (a) Viewed along the *a*-axis. (b) Viewed along the *c*-axis. Dashed lines denote intermolecular hydrogen bonds.

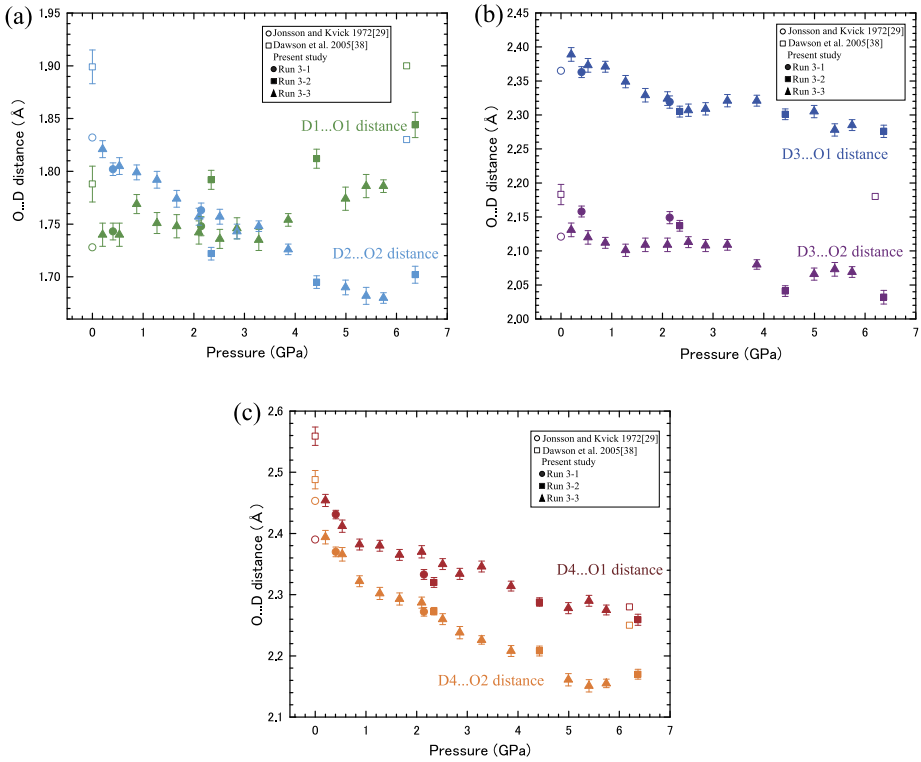

FIG. 6. Pressure-induced changes in the D···O distances of the intermolecular hydrogen bonds. (a) D1···O1 distance and D2···O2 distance of the N–D···O bonds. (b) D3···O1 distance and D3···O2 distance of the bifurcated N–D···O bond. (c) D4···O1 distance and D4···O2 distance of the bifurcated C–D···O bond.

at 0.2 GPa to 160.4° at 6.4 GPa. In contrast, the D2···O2 distance and the N···O2 distance decrease with increasing pressure from 0.2 GPa to 6.4 GPa. Although the D1···O1 distance is the shortest among the intermolecular D···O distances at ambient pressure, the D1···O1 and D2···O2 distances become almost equal at ∼3 GPa. Above 3 GPa, the D2···O2 distance becomes the shortest of the D···O distances.

The layers of the molecules are stacked along the *b*-axis, and two types of bifurcated hydrogen bonds are found to alternate between the layers [Fig. 5(b)]. One is a pair of N–D3···O1 and N–D3···O2 bonds and the other is a pair of C2–D4···O1 and C2–D4···O2 bonds. Figure 6(b) shows the pressure dependences of the intermolecular D3···O1 distances and D3···O2 distance of the bifurcated hydrogen bond. Both of the D3···O1 and the D3···O2 distances decrease with increasing pressure, in contrast to the result of the previous single-crystal X-ray diffraction study, in which no significant change of the D3···O1 and D3···O2 distances was observed.[38] The D3···O1 and the D3···O2 distances are decreased by 7.0% and 2.8%, respectively, from 0.2 GPa to 6.4 GPa. The N–D3 distance is almost constant, while the N···O1 and N···O2 distances decrease during compression (see Table IV), in contrast to those observed in the *ac* plane. Figure 6(c) shows the pressure dependence of the intermolecular D···O distance of the bifurcated C–D···O bonds. Both the D4···O1 and the D4···O2 distances decrease with increasing pressure. The D4···O1 and the D4···O2 distances are compressed by 6.7% and 8.1%, respectively, from 0.2 to 6.4 GPa. The C–D4 distance is almost constant, and the C···O1 and the C···O2 distances decrease with pressure (Table IV); this is similar to that observed in the bifurcated D3···O1 and D3···O2 bonds.

IV. DISCUSSION

The X-ray and neutron diffraction measurements on deuterated α-glycine at high pressure and room temperature indicate that there is no structural phase transition, at least up to 8.7 GPa. The cell parameters and unit cell volume decrease continuously with increasing pressure, while no significant changes are observed in the intramolecular bond lengths and the bond angles, suggesting that the changes in the intermolecular distances induce the pressure change of the lattice parameters. Effects of isotopic substitution of deuterium atoms for hydrogen atoms on phase changes, and molecular arrangement in solid phase, the so-called Ubbelohde effect, have been reported on some molecular crystals containing short hydrogen bonding (i.e., Refs. 59–61). In contrast, the Ubbelohde effect on α-glycine under high pressure has not been found by Raman measurements,[40] as well as that on γ-glycine.[62] The compressibility and the intramolecular distance are compared between non-deuterated α-glycine[38] and deuterated α-glycine (Fig. 4 and Table III, respectively), while no significant changes induced by the deuteration are observed.

The various intermolecular hydrogen bonds behave differently upon compression. The intermolecular distance simply decreases with increasing pressure in the case of the bifurcated N–D3···O1 and N–D3···O2 hydrogen bonds, and the bifurcated C2–D4···O1 and C2–D4···O2 hydrogen bonds, which are formed in between the layers of the molecules stacked along the *b*-axis. These hydrogen bonds are relatively weak, and therefore large voids are considered to be formed between the molecules. Upon compression, the layers are likely to approach closer with decreasing the D···O distance of the bifurcated bonds, which induce the largest compressibility of the *b*-axis.

TABLE IV. Geometry for the intermolecular distance and angles of deuterated α-glycine at representative pressure.

N/C–D···O	Pressure (GPa)	N/C···O (Å)	N/C–D (Å)	D···O (Å)	N/C–D···O (deg)
N–D1···O1	0.2	2.780 (10)	1.054 (8)	1.740 (11)	168.8 (6)
	1.3	2.789 (9)	1.053 (9)	1.751 (10)	167.6 (6)
	2.2	2.775 (5)	1.044 (6)	1.748 (9)	166.8 (4)
	3.9	2.756 (5)	1.020 (6)	1.754 (6)	166.3 (4)
	4.4	2.785 (8)	1.000 (7)	1.812 (9)	163.4 (5)
	5.7	2.768 (5)	1.006 (6)	1.786 (6)	164.6 (4)
	6.4	2.814 (6)	1.008 (7)	1.844 (12)	160.4 (5)
N–D2···O2	0.2	2.843 (7)	1.032 (7)	1.821 (8)	170.4 (7)
	1.3	2.812 (6)	1.027 (7)	1.792 (8)	171.5 (6)
	2.2	2.787 (5)	1.026 (5)	1.763 (7)	175.1 (4)
	3.9	2.773 (4)	1.051 (5)	1.726 (5)	174.6 (4)
	4.4	2.742 (5)	1.050 (6)	1.695 (6)	173.9 (5)
	5.7	2.750 (4)	1.072 (5)	1.680 (7)	175.6 (4)
	6.4	2.754 (5)	1.054 (6)	1.702 (8)	175.4 (5)
N–D3···O1	0.2	2.956 (8)	1.005 (10)	2.389 (10)	114.9 (7)
	1.3	2.910 (8)	1.024 (8)	2.349 (9)	113.3 (6)
	2.2	2.895 (7)	1.003 (7)	2.319 (8)	115.6 (3)
	3.9	2.853 (6)	1.016 (7)	2.321 (8)	111.4 (3)
	4.4	2.810 (6)	1.007 (7)	2.301 (8)	110.0 (5)
	5.7	2.792 (7)	1.002 (8)	2.285 (8)	110.1 (2)
	6.4	2.748 (8)	0.995 (8)	2.276 (9)	107.8 (3)
N–D3···O2	0.2	3.073 (8)		2.131 (10)	155.4 (8)
	1.3	3.064 (8)		2.101 (9)	155.9 (7)
	2.2	3.081 (6)		2.149 (9)	153.8 (4)
	3.9	3.047 (7)		2.080 (7)	157.8 (3)
	4.4	2.997 (6)		2.041 (8)	157.8 (6)
	5.7	3.025 (7)		2.069 (8)	158.8 (3)
	6.4	2.988 (8)		2.032 (10)	160.2 (3)
C–D4···O1	0.2	3.339 (9)	1.065 (10)	2.454 (10)	140.0 (7)
	1.3	3.256 (9)	1.068 (9)	2.380 (9)	138.4 (7)
	2.2	3.221 (8)	1.088 (9)	2.333 (8)	137.6 (3)
	3.9	3.177 (8)	1.066 (8)	2.314 (8)	137.9 (6)
	4.4	3.159 (7)	1.068 (8)	2.288 (7)	137.5 (6)
	5.7	3.147 (8)	1.068 (8)	2.275 (8)	137.3 (3)
	6.4	3.116 (8)	1.053 (8)	2.259 (9)	137.3 (3)
C–D4···O2	0.2	3.258 (9)		2.394 (11)	137.6 (8)
	1.3	3.159 (9)		2.302 (10)	136.0 (7)
	2.2	3.125 (7)		2.272 (7)	133.8 (4)
	3.9	3.057 (8)		2.208 (9)	135.1 (6)
	4.4	3.045 (8)		2.208 (8)	133.7 (6)
	5.7	2.992 (8)		2.155 (7)	133.5 (6)
	6.4	2.993 (8)		2.170 (8)	133.4 (4)

By contrast, an increase of the D1···O1 distance with compression is observed [see Fig. 6(a)]. The D1···O1 distance is 1.728 Å at ambient pressure,[29] which is short when compared to distances in other organic compounds in the "amino acids, peptides, and complexes" category of the Cambridge Structural Database.[14] The N–D1 distance of α-glycine is 1.054 Å at ambient pressure,[29] which is significantly longer than a typical N–H bond length in the Cambridge Database default values (1.009 Å).[63] Thus, the intramolecular N–D1 distance decreases during the compression accompanied by bending of the N–D1···O1 angle and consequent increase of the intermolecular D1···O1 distance. The D2···O2 and N···O2 distances decrease during compression; above 3 GPa, D2···O2 becomes the shortest of the D···O distances. Around 3 GPa, some kind of structural rearrangement was suggested by the changes in the pressure-dependence of the COO^- and NH_3^+ vibration frequencies.[39,40] The behavior of the N–D1···O1 and N–D2···O2 bonds would induce a relatively small compressibility of the c'-axis and a-axis, respectively.

The Hirshfeld surface is constructed by partitioning the space in the crystal structure into regions where the electron density distribution of a sum of spherical atoms for the molecule (i.e., promolecule) dominates the corresponding sum of the electron density of the crystal (i.e., procrystal).[64,65] In this study, the Hirshfeld surface of α-glycine at each pressure is calculated and visualized using the program *CrystalExplorer*.[66] The distance from the surface to the nearest atom in another molecule and the distance from the surface to the

nearest atom in the molecule itself are defined as d_e and d_i, respectively.[64] A plot of d_e against d_i is called the "fingerprint plot," which is a useful tool to directly compare the packing of 3-D molecules in a 2-D graph. Figures 7(a) and 7(b) show the fingerprint plots for α-glycine at 0.2 GPa and 6.4 GPa, respectively. A diffuse region is seen at the long d_e and d_i regions in the plot at 0.2 GPa, indicating the existence of voids in the structure [region 1 in Fig. 7(a)]. The diffuse region decreases at 6.4 GPa, suggesting the reduction of the void space with compression. On the other hand, the "spikes" originating from D···O bonds are observed in the small d_e and d_i region (region 2 in Fig. 7). The position of the tip of the spikes is hardly shift with compression; however the origin of the tip of the spikes changes from the D1···O1 bond at 0.2 GPa to the D2···O2 bond at 6.4 GPa. The results suggest that the strong N–D1···O1 bonds and N–D2···O2 bonds are less compressible, while weak contacts between the molecules and the void regions in the crystal decrease with compression. The presence of H···H contacts is represented by the diagonal region (region 3 in Fig. 7); a slight change in the position and shape is observed with compression. A similar pressure-induced behavior in the intermolecular interactions was reported in other amino acids, such as L-alanine[13] and α-glycylglycine.[67] The results of Hirshfeld surface analysis show that the shortest H···H contact of the d_e + d_i distance at 6.4 GPa is much longer than the lower limit proposed in organic structures, 1.7 Å.[68] The shortest D···O distance of α-glycine at 6.4 GPa is 1.702 Å, which is longer than that of L-alanine and the high pressure phase of L-serine at a similar pressure.[12,19] These results imply that α-glycine can maintain its crystal structure at higher pressures than the pressure range of the present study.

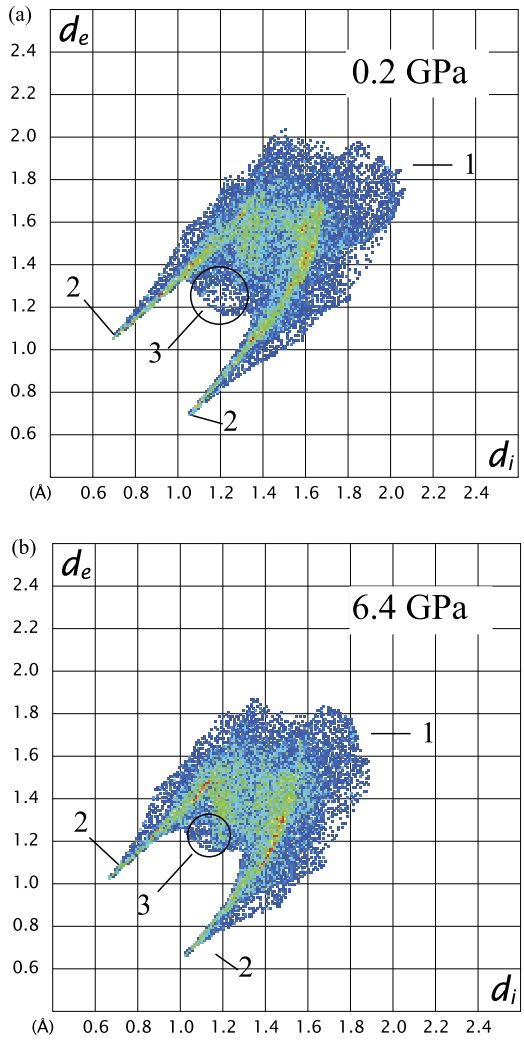

FIG. 7. Fingerprint plots at (a) 0.2 GPa and (b) 6.4 GPa. (1) Diffuse region, (2) spikes of N–D···O hydrogen bonds, and (3) the shortest H···H contacts.

V. CONCLUSION

Powder XRD measurements on deuterated α-glycine indicated that there is no phase change up to 8.7 GPa, while anisotropic compression of the crystal structure was observed. Single-crystal XRD measurements at 4.1 GPa indicated that the intramolecular bond distances and angles hardly change with compression. Changes of the intermolecular distance were investigated by powder neutron diffraction measurements up to 6.4 GPa. An increase of the D1···O1 distance with compression was found. The D2···O2 distance decreased with increasing pressure and became the shortest of the D···O distances above 3 GPa. The behavior of the D1···O1 and D2···O2 bonds would induce a relatively small compressibility of the c'-axis and a-axis, respectively. The layers of the molecules in the *ac*-plane are stacked along the *b*-axis, and bifurcated N–D3···O1 and N–D3···O2 bonds and bifurcated C–D4···O1 and C–D4···O2 bonds form between the layers. A large decrease in the D···O distances of the bifurcated N–D···O and the C–D···O bonds between the layers was observed, which manifests in the largest compressibility of the *b*-axis. The Hirshfeld analysis suggests that compression would lead to the decrease of the void region in the crystal rather than the shrinkage of robust hydrogen bonds.

ACKNOWLEDGMENTS

Powder X-ray and neutron diffraction experiments were performed through the PF (Nos. 2014G695 and 2015G694) and the J-PARC user programs (Nos. 2015A0265 and 2016A0195), respectively. This work was supported by JSPS KAKENHI Grant Nos. 25287147, 15K13600, 15H05828, 16K17839, and 26246039.

[1] K. Aoki, S. Usuba, M. Yoshida, Y. Kakudate, K. Tanaka, and S. Fujiwara, J. Chem. Phys. **89**, 529 (1988).
[2] E. V. Boldyreva, T. N. Drebushchak, T. P. Shakhtshneider, H. Sowa, H. Ahsbahs, S. V. Goryainov, S. N. Ivashevskaya, E. N. Kolesnik, V. A. Drebushchak, and E. B. Burgina, Arkivoc **12**, 128 (2004).
[3] L. Ciabini, M. Santoro, F. A. Gorelli, R. Bini, V. Schettino, and S. Raugei, Nat. Mater. **6**, 39 (2007).
[4] E. V. Boldyreva, Acta Crystallogr., Sect. A: Found. Crystallogr. **64**, 218 (2008).
[5] K. Wang, D. F. Duan, R. Wang, A. L. Lin, Q. L. Cui, B. B. Liu, T. Cui, B. Zou, X. Zhang, J. Z. Hu, G. T. Zou, and H. K. Mao, Langmuir **25**, 4787 (2009).
[6] A. Shinozaki, N. Noguchi, and H. Kagi, Chem. Phys. Lett. **574**, 66 (2013).
[7] G. Resnati, E. Boldyreva, P. Bombicz, and M. Kawano, IUCrJ **2**, 675 (2015).
[8] X. Tan, K. Wang, T. T. Yan, X. D. Li, J. Liu, K. Yang, B. B. Liu, G. T. Zou, and B. Zou, J. Phys. Chem. C **119**, 10178 (2015).
[9] E. Patyk, A. Jenczak, and A. Katrusiak, Phys. Chem. Chem. Phys. **18**, 11474 (2016).
[10] C. H. Gorbitz, Acta Crystallogr., Sect. B: Struct. Sci. **66**, 84 (2010).
[11] C. H. Gorbitz, Crystallogr. Rev. **21**, 160 (2015).

[12]N. P. Funnell, A. Dawson, D. Francis, A. R. Lennie, W. G. Marshall, S. A. Moggach, J. E. Warren, and S. Parsons, CrystEngComm **12**, 2573 (2010).
[13]N. A. Tumanov, E. V. Boldyreva, B. A. Kolesov, A. V. Kurnosov, and R. Q. Cabrera, Acta Crystallogr., Sect. B: Struct. Sci. **66**, 458 (2010).
[14]N. P. Funnell, W. G. Marshall, and S. Parsons, CrystEngComm **13**, 5841 (2011).
[15]N. A. Tumanov and E. V. Boldyreva, Acta Crystallogr., Sect. B: Struct. Sci. **68**, 412 (2012).
[16]E. N. Kolesnik, S. V. Goryainov, and E. V. Boldyreva, Dokl. Phys. Chem. **404**, 169 (2005).
[17]S. A. Moggach, D. R. Allan, C. A. Morrison, S. Parsons, and L. Sawyer, Acta Crystallogr., Sect. B: Struct. Sci. **61**, 58 (2005).
[18]E. V. Boldyreva, H. Sowa, Y. V. Seryotkin, T. N. Drebushchak, H. Ahsbahs, V. Chernyshev, and V. Dmitriev, Chem. Phys. Lett. **429**, 474 (2006).
[19]P. A. Wood, D. Francis, W. G. Marshall, S. A. Moggach, S. Parsons, E. Pidcock, and A. L. Rohl, CrystEngComm **10**, 1154 (2008).
[20]B. A. Zakharov, B. A. Kolesov, and E. V. Boldyreva, Acta Crystallogr., Sect. B: Struct. Sci. **68**, 275 (2012).
[21]S. A. Moggach, D. R. Allan, S. J. Clark, M. J. Gutmann, S. Parsons, C. R. Pulham, and L. Sawyer, Acta Crystallogr., Sect. B: Struct. Sci. **62**, 296 (2006).
[22]V. S. Minkov, A. S. Krylov, E. V. Boldyreva, S. V. Goryainov, S. N. Bizyaev, and A. N. Vtyurin, J. Phys. Chem. B **112**, 8851 (2008).
[23]V. S. Minkov, S. V. Goryainov, E. V. Boldyreva, and C. H. Gorbitz, J. Raman Spectrosc. **41**, 1748 (2010).
[24]V. S. Minkov, N. A. Tumanov, R. Q. Cabrera, and E. V. Boldyreva, CrystEngComm **12**, 2551 (2010).
[25]C. Fujimoto, A. Shinozaki, K. Mimura, T. Nishida, H. Gotou, K. Komatsu, and H. Kagi, Chem. Commun. **51**, 13358 (2015).
[26]S. Takahashi, H. Kagi, C. Fujimoto, A. Shinozaki, H. Gotou, T. Nishida, and K. Mimura, Chem. Lett. **46**, 334 (2017).
[27]G. Albrecht and R. B. Corey, J. Am. Chem. Soc. **61**, 1087 (1939).
[28]R. E. Marsh, Acta Crystallogr. **11**, 654 (1958).
[29]P. G. Jonsson and A. Kvick, Acta Crystallogr., Sect. B: Struct. Sci. **28**, 1827 (1972).
[30]L. F. Power, K. E. Turner, and F. H. Moore, Acta Crystallogr., Sect. B: Struct. Sci. **32**, 11 (1976).
[31]E. V. Boldyreva, H. Ahsbahs, and H. P. Weber, Z. Kristallogr. - Cryst. Mater. **218**, 231 (2003).
[32]Y. Iitaka, Acta Crystallogr. **13**, 35 (1960).
[33]T. N. Drebushchak, E. V. Boldyreva, and E. S. Shutova, Acta Crystallogr., Sect. E: Struct. Rep. Online **58**, o634 (2002).
[34]S. Chongprasert, S. A. Knopp, and S. L. Nail, J. Pharm. Sci. **90**, 1720 (2001).
[35]E. V. Boldyreva, V. A. Drebushchak, T. N. Drebushchak, I. E. Paukov, Y. A. Kovalevskaya, and E. S. Shutova, J. Therm. Anal. Calorim. **73**, 409 (2003).
[36]E. V. Boldyreva, V. A. Drebushchak, T. N. Drebushchak, I. E. Paukov, Y. A. Kovalevskaya, and E. S. Shutova, J. Therm. Anal. Calorim. **73**, 419 (2003).
[37]Y. Iitaka, Acta Crystallogr. **14**, 1 (1961).
[38]A. Dawson, D. R. Allan, S. A. Belmonte, S. J. Clark, W. I. F. David, P. A. McGregor, S. Parsons, C. R. Pulham, and L. Sawyer, Cryst. Growth Des. **5**, 1415 (2005).
[39]C. Murli, S. M. Sharma, S. Karmakar, and S. K. Sikka, Phys. B **339**, 23 (2003).
[40]B. B. Sharma, C. Murli, R. Chitra, and S. M. Sharma, J. Raman Spectrosc. **43**, 138 (2012).
[41]H. N. Bordallo, E. V. Boldyreva, A. Buchsteiner, M. M. Koza, and S. Landsgesell, J. Phys. Chem. B **112**, 8748 (2008).
[42]S. V. Goryainov, E. N. Kolesnik, and E. Boldyreva, Phys. B **357**, 340 (2005).
[43]E. V. Boldyreva, S. N. Ivashevskaya, H. Sowa, H. Ahsbahs, and H. P. Weber, Dokl. Phys. Chem. **396**, 111 (2004).
[44]E. V. Boldyreva, S. N. Ivashevskaya, H. Sowa, H. Ahsbahs, and H. P. Weber, Z. Kristallogr. - Cryst. Mater. **220**, 50 (2005).
[45]S. A. Moggach, W. G. Marshall, D. M. Rogers, and S. Parsons, CrystEng Comm **17**, 5315 (2015).
[46]S. V. Goryainov, E. Boldyreva, and E. N. Kolesnik, Chem. Phys. Lett. **419**, 496 (2006).
[47]C. L. Bull, G. Flowitt-Hill, S. de Gironcoli, E. Kucukbenli, S. Parsons, C. H. Pham, H. Y. Playford, and M. G. Tucker, IUCrJ **4**, 569 (2017).
[48]H. Mao, P. Bell, J. W. Shaner, and D. Steinberg, J. Appl. Phys. **49**, 3276 (1978).
[49]Y. Seto, D. Nishio-Hamane, T. Nagai, and N. Sata, Rev. High Pressure Sci. Technol. **20**, 269 (2010).
[50]B. H. Toby, J. Appl. Crystallogr. **34**, 210 (2001).
[51]T. Hattori, A. Sano-Furukawa, H. Arima, K. Komatsu, A. Yamada, Y. Inamura, T. Nakatani, Y. Seto, T. Nagai, W. Utsumi, T. Iitaka, H. Kagi, Y. Katayama, T. Inoue, T. Otomo, K. Suzuya, T. Kamiyama, M. Arai, and T. Yagi, Nucl. Instrum. Methods Phys. Res., Sect. A **780**, 55 (2015).
[52]S. Klotz, G. Hamel, and J. Frelat, High Pressure Res. **24**, 219 (2004).
[53]R. Iizuka, T. Yagi, H. Gotou, K. Komatsu, and H. Kagi, High Pressure Res. **32**, 430 (2012).
[54]K. Momma and F. Izumi, J. Appl. Crystallogr. **44**, 1272 (2011).
[55]P. Vinet, J. H. Rose, J. Ferrante, and J. R. Smith, J. Phys.: Condens. Matter **1**, 1941 (1989).
[56]F. Birch, Phys. Rev. **71**, 809 (1947).
[57]P. Lozano-Casal, D. R. Allan, and S. Parsons, Acta Crystallogr., Sect. B: Struct. Sci. **64**, 466 (2008).
[58]J. Bernstein, R. E. Davis, L. Shimoni, and N. L. Chang, Angew. Chem., Int. Ed. **34**, 1555 (1995).
[59]J. M. de Souza, P. T. C. Freire, H. N. Bordallo, and D. N. Argyriou, J. Phys. Chem. B **111**, 5034 (2007).
[60]K. Merz and A. Kupka, Cryst. Growth Des. **15**, 1553 (2015).
[61]A. R. Ubbelohde, J. Chim. Phys. Phys.-Chim. Biol. **46**, 429 (1949).
[62]A. K. Mishra, C. Murli, and S. M. Sharma, J. Phys. Chem. B **112**, 15867 (2008).
[63]T. S. Gautam and R. Desiraju, *The Weak Hydrogen Bond: In Structural Chemistry and Biology*, IUCr Monographs on Crystallography Vol. 9 (Oxford Science Publication, 1999).
[64]J. J. McKinnon, M. A. Spackman, and A. S. Mitchell, Acta Crystallogr., Sect. B: Struct. Sci. **60**, 627 (2004).
[65]M. A. Spackman and D. Jayatilaka, CrystEngComm **11**, 19 (2009).
[66]S. K. Wolff, D. J. Grimwood, J. J. McKinnon, J. Turner, D. Jayatilaka, and M. A. Spackman, CrystalExplorer version 3.1, University of Western Australia, http://hirshfeldsurface.net, 2005.
[67]S. A. Moggach, D. R. Allan, S. Parsons, and L. Sawyer, Acta Crystallogr., Sect. B: Struct. Sci. **62**, 310 (2006).
[68]P. A. Wood, J. J. McKinnon, S. Parsons, E. Pidcock, and M. A. Spackman, CrystEngComm **10**, 368 (2008).